

Impact of the range of the interaction on the quantum dynamics of a bosonic Josephson junction

Sudip Kumar Haldar^{a,b,*}, Ofir E. Alon^{a,b}

^aDepartment of Mathematics, University of Haifa, Haifa 3498838, Israel

^bHaifa Research Center for Theoretical Physics and Astrophysics, University of Haifa, Haifa 3498838, Israel

Abstract

The out-of-equilibrium quantum dynamics of a bosonic Josephson junction (BJJ) with long-range interaction is studied in real space by solving the time-dependent many-body Schrödinger equation numerically accurately using the multiconfigurational time-dependent Hartree method for bosons. Having the many-boson wave-function at hand we can examine the impact of the range of the interaction on the properties of the BJJ dynamics, viz. density oscillations and their collapse, self trapping, depletion and fragmentation, as well as the position variance, both at the mean-field and many-body level. Explicitly, the frequency of the density oscillations and the time required for their collapse, the value of fragmentation at the plateau, the maximal and the minimal values of the position variance in each cycle of oscillation and the overall pace of its growth are key to our study. We find competitive effect between the interaction and the confining trap. The presence of the tail part of the interaction basically enhances the effective repulsion as the range of the interaction is increased starting from a short, finite range. But, as the range becomes comparable with the trap size, the system approaches a situation where all the atoms feel a constant potential and the impact of the tail on the dynamics diminishes. There is an optimal range of the interaction in which physical quantities of the junction are attaining their extreme values.

1. Introduction

The recent advancements in experimental techniques for interacting Bose gas have made it possible to study the quantum many-body dynamics in a highly controllable manner [1]. In this connection, the dynamics of many-body tunneling [2] is one of the most fundamental problem. A Bose-Einstein condensate (BEC) of interacting dilute Bose gas in a double well, which is generally referred to as a bosonic Josephson junction (BJJ) [3], provides a unique opportunity to study many-body tunneling dynamics. Naturally, the dynamics of BJJs have attracted a lot of attention both theoretically and experimentally [3, 4, 5, 6, 7, 8, 9, 10, 11, 12, 13, 14, 15, 16, 17, 18, 19, 20, 21, 22, 23, 24]. Explicitly, Josephson oscillations [3, 5, 6, 19, 22, 23], collapse and revival cycles [4], self trapping (suppression of tunneling) [3, 4, 5, 6, 19], fragmentation [20] and more recently the variances and uncertainty product of the many-body position and momentum operators [21] have been studied. Note that while tunneling, self trapping and Josephson oscillations have some explanations at the mean-field level, the collapse and revival and fragmentation dynamics require many-body treatments like the Bose-Hubbard model [12] or even solving the full many-body Schrödinger equation [17, 25]. A universality has been predicted in the fragmentation dynamics in the sense that systems consisting of different numbers of particles fragment to the same value for the

same mean-field interaction parameter [20]. However, it has been shown that even when the Bose-Hubbard model is apparently applicable, the full many-body Schrödinger equation can grab new features. For example, there is a symmetry in the Bose-Hubbard Hamiltonian with respect to repulsive and attractive interactions of equal magnitude. Such symmetry implies an equivalence between the time evolution of the survival probability and the fragmentation of a repulsive and an attractive BJJ with equal magnitude of the strength of the interaction. However, no such symmetry exists at the level of the full many-body Hamiltonian [18].

So far, only contact interactions between the atoms have been considered in the study of BJJs [17, 18, 20, 22, 23]. Actually, contact δ -interaction is widely used in the theoretical studies of trapped ultra-cold atomic gases [1]. However, in many recent experiments with the ultra-cold dipolar atoms ^{52}Cr [26, 27], ^{164}Dy [28] and ^{168}Er [29], it has been shown that the short-range inter-particle interaction potential is not enough to account for the observed physics and an additional long-range term is needed to describe the overall two-body interaction, see also the reviews [30, 31]. It is also possible, in experiments, to tune the strength of the dipolar interactions including its sign by using a rotating polarizing field [32]. For a ^{52}Cr BEC, one can also use the Feshbach resonance to tune the s -wave scattering length [33], and this has already been used to enhance the dipolar effects in a BEC [34]. Naturally, the question arises what role the range of the interaction plays and how that affects our present understanding of the physics of an ultra-cold Bose gas.

To address these questions, several static properties includ-

*Corresponding author.

Email addresses: shaldar@campus.haifa.ac.il (Sudip Kumar Haldar), ofir@research.haifa.ac.il (Ofir E. Alon)

ing the fragmentation of the ground state of the trapped ultra-cold bosonic atoms with long-range interaction have already been studied theoretically in one, two and three spatial dimensions [35, 36, 37]. Also, the non-equilibrium dynamics of trapped bosons interacting by a long-range interaction has been studied both at the mean-field level [30, 31, 38, 39] as well as the many-body level [40]. However, all these studies considered mainly a single trap of various geometries.

Therefore, in this work, we would like to bring together the topics of BJJs and long-range interactions. We numerically study the tunnelling dynamics of a BEC with a tunable long-range interactions in a double well. Here we are interested in the generic behaviour of the quantum many-body dynamics with a finite-range inter-atomic interaction. The physics of the many-body dynamics is not expected to vary qualitatively with the shape of the interactions provided the strength and range of the interaction remain the same. In this work we consider a model interaction $W(r) = \frac{\lambda_0}{\sqrt{(r/D)^{2n} + 1}}$ of strength λ_0 , half-width D with $n = 3$ and r being the inter-particle separation. In our study, we will vary D for fixed values of λ_0 . Such interactions appear naturally in the so called ‘‘Rydberg-dressed’’ ultra-cold systems which are studied in recent experiments [41, 42]. Moreover, at large r , $r/D \gg 1$, such interactions behave as a dipolar interaction which is relevant for dipolar ultra-cold atoms [30, 31]. On the other hand, at small r ($r/D \ll 1$), $W(r)$ reduces to a soft sphere interaction and has many similar effects as the usual δ -interaction.

In our studies below, starting with a short range, we tune the effective range of the interaction. We observe that the presence of the long-range tail in the inter-particle interaction potential basically enhances the effect of the interaction until the range of the interaction becomes comparable with the inter-well separation. Also, for the stronger interaction, the range of the interaction plays a more prominent role. Already at the mean-field level, we observe clear effect on the Josephson oscillation frequency and amplitude for a sufficiently strong interaction strength. Naturally, the many-body dynamics is even richer. The loss of coherence and development of correlations and fragmentation are significantly affected due to the presence of the long-range tail in the inter-particle interaction potential which in turn alters the usual collapse of oscillations of the survival probability and self trapping. Variances of operators which, unlike other quantities, depend on the actual number of depleted atoms and not on the condensate fraction are a very sensitive measure of correlations. In the infinite-particle limit, as the depletion tends to zero and the energy per particle and density per particle of a condensate overlaps with those obtained from a mean-field theory, variances of operators can show significantly different behaviour which can only be obtained with a many-body theory. Naturally, in this case also, the variance reveals more prominent effect of the long-range behavior.

This paper is organised as follows. In Sec. 2, we introduce the in principle numerically-exact many-body method used to solve the time-dependent many-body Schrödinger equation. In sec. 3 we discuss our findings and finally conclusions are drawn

in Sec. 4. The Appendix puts forward additional numerical details.

2. Theoretical framework

The time evolution of N interacting structureless bosons is governed by the time-dependent many-body Schrödinger equation:

$$\hat{H}\Psi = i\frac{\partial\Psi}{\partial t}, \quad \hat{H}(\mathbf{r}_1, \mathbf{r}_2, \dots, \mathbf{r}_N) = \sum_{j=1}^N \hat{h}(\mathbf{r}_j) + \sum_{k>j=1}^N W(\mathbf{r}_j - \mathbf{r}_k), \quad (1)$$

where $\hat{h} = 1$, \mathbf{r}_j is the coordinate of the j -th boson, $\hat{h}(\mathbf{r}) = \hat{T}(\mathbf{r}) + V(\mathbf{r})$ is the one-body Hamiltonian containing kinetic and potential energy terms, and $W(\mathbf{r}_j - \mathbf{r}_k)$ is the pairwise interaction between the j -th and k -th bosons. The time-dependent many-boson Schrödinger equation (1) cannot be solved exactly (analytically), except for a few specific cases only, see, e.g., [43]. Hence, an in principle numerically-exact many-body method for identical bosons, based on the multi-configurational time-dependent Hartree (MCTDH) [44, 45] method, viz. the multi-configurational time-dependent Hartree method for bosons (MCTDHB), was developed to solve Eq. (1). Detailed derivation of the MCTDHB equation of motions can be found in [46, 47]. Below we briefly describe the basic idea behind the method.

In MCTDHB, the ansatz for solving Eq. (1) is taken as the superposition of all $\binom{N+M-1}{N}$ time-dependent permanents obtained by distributing N bosons in M single-particle orbitals. Thus, the many-body wavefunction $\Psi(t)$ is given by

$$|\Psi(t)\rangle = \sum_{\vec{n}} C_{\vec{n}}(t) |\vec{n}; t\rangle, \quad (2)$$

where the summation runs over all possible configurations whose occupations \vec{n} preserve the total number of bosons N . The time-dependent permanents are given by

$$|\vec{n}; t\rangle = \frac{1}{\sqrt{n_1! n_2! \dots n_M!}} (b_1^\dagger(t))^{n_1} (b_2^\dagger(t))^{n_2} \dots (b_M^\dagger(t))^{n_M} |vac\rangle, \quad (3)$$

where $\vec{n} = (n_1, n_2, \dots, n_M)$ represents the occupations of the orbitals such that $n_1 + n_2 + \dots + n_M = N$, and $|vac\rangle$ is the vacuum. The bosonic annihilation and corresponding creation operators obey the usual commutation relations $b_k(t)b_j^\dagger(t) - b_j^\dagger(t)b_k(t) = \delta_{kj}$ at any point in time. Note that in representation (2) both the expansion coefficients $\{C_{\vec{n}}(t)\}$ and orbitals $\{\phi_k(\mathbf{r}, t)\}$ comprising the permanents $|\vec{n}; t\rangle$ are independent parameters. Throughout this work we have performed all computations with $M = 2$ orbitals. The results are found to be accurate for the quantities and propagation times considered here. For further details on numerical computations and its accuracy, we refer the reader to the Appendix.

To solve for the time-dependent wavefunction $\Psi(t)$ we need to determine the evolution of the coefficients $\{C_{\vec{n}}(t)\}$ and orbitals $\{\phi_k(\mathbf{r}, t)\}$ with time. To derive the equations of motion

governing the evolution of $\{C_{\vec{n}}(t)\}$ and $\{\phi_k(\mathbf{r}, t)\}$, we employ the usual Lagrangian formulation of the time-dependent variational principle [48, 49] subject to the orthonormality between the orbitals. In this framework, we substitute the many-body *ansatz* (2) for $\Psi(t)$ into the functional action of the time-dependent Schrödinger equation which reads:

$$S[\{C_{\vec{n}}(t)\}, \{\phi_k(\mathbf{r}, t)\}] = \int dt \left\{ \left\langle \Psi \left| \hat{H} - i \frac{\partial}{\partial t} \right| \Psi \right\rangle - \sum_{k,j}^M \mu_{kj}(t) [\langle \phi_k | \phi_j \rangle - \delta_{kj}] \right\}. \quad (4)$$

The time-dependent Lagrange multipliers $\mu_{kj}(t)$ ensure that the time-dependent orbitals $\phi_k(\mathbf{r}, t)$ remain orthonormal throughout the propagation [47]. The next step is to require stationarity of the functional action with respect to its arguments $\{C_{\vec{n}}(t)\}$ and $\{\phi_k(\mathbf{r}, t)\}$. This variation is performed separately for the coefficients and for the orbitals, recalling that they are independent variational parameters. After a lengthy but straightforward calculation we arrive at the final equations of motion which read for the orbitals $\phi_j(\mathbf{r}, t)$, $j = 1, \dots, M$:

$$i |\dot{\phi}_j\rangle = \hat{\mathbf{P}} \left[\hat{h} |\phi_j\rangle + \sum_{k,s,q,l=1}^M \{\rho(t)\}_{jk}^{-1} \rho_{ksql} \hat{W}_{sl} |\phi_q\rangle \right],$$

$$\hat{\mathbf{P}} = 1 - \sum_{j=1}^M |\phi_j\rangle \langle \phi_j|. \quad (5)$$

Here $\rho(t)$ is the reduced one-body density matrix and $\rho_{ksql} = \langle \Psi | b_k^\dagger b_s^\dagger b_q b_l | \Psi \rangle$ are the elements of the reduced two-body density matrix. Given the (normalized) wavefunction $\Psi(t)$, the reduced one-body density matrix is given by

$$\begin{aligned} \rho(\mathbf{r}_1 | \mathbf{r}'_1; t) &= N \int d\mathbf{r}_2 \dots d\mathbf{r}_N \Psi^*(\mathbf{r}'_1, \mathbf{r}_2, \dots, \mathbf{r}_N; t) \\ &\quad \times \Psi(\mathbf{r}_1, \mathbf{r}_2, \dots, \mathbf{r}_N; t) \\ &= \sum_{j=1}^M n_j(t) \phi_j^{*NO}(\mathbf{r}'_1, t) \phi_j^{NO}(\mathbf{r}_1, t). \end{aligned} \quad (6)$$

The quantities $\phi_j^{NO}(\mathbf{r}_1, t)$ are the natural orbitals and $n_j(t)$ the natural occupation numbers which are time-dependent and used to define the (time varying) degree of condensation in a system of interacting bosons [50]. The natural occupations satisfy $\sum_{j=1}^M n_j = N$ and if only one macroscopic eigenvalue $n_1(t) \approx O(N)$ exists, the system is condensed [50] whereas if there are more than one macroscopic eigenvalues, the BEC is said to be fragmented [25, 51, 52, 53, 54]. The microscopic occupations in the higher orbitals $f = \sum_{j=2}^M \frac{n_j}{N}$ for a condensate is known as the depletion per particle. On the other hand, the macroscopic occupation of a higher natural orbital, viz. $\frac{n_{j>1}}{N}$ where $n_j \approx O(N)$, is called fragmentation. Thus, it is quite obvious that for $M = 2$ orbitals, both the depletion and fragmentation basically have the same mathematical expression (but different physical interpretations) and, hence, for the ease of our discussion, below we refer to both of them by f . The density of the system is the diagonal of the reduced one-body density matrix, $\rho(\mathbf{r}; t) = \rho(\mathbf{r} | \mathbf{r}; t)$.

The equations of motion for the propagation of the coefficients is given by

$$\mathbf{H}(t)\mathbf{C}(t) = i \frac{\partial \mathbf{C}(t)}{\partial t}, \quad (7)$$

where $\mathbf{H}(t)$ is the Hamiltonian matrix with the elements $H_{\vec{n}\vec{n}'}(t) = \langle \vec{n}; t | \hat{H} | \vec{n}'; t \rangle$. Recently a parallel version of MCTDHB has been implemented using a novel mapping technique [55]. We note that by propagating in imaginary time the MCTDHB equations also allow one to determine the ground state of interacting many-boson systems, see [25].

3. Results

In this section we discuss the findings of our study of the dynamics of a BEC in a one dimensional (1D) symmetric double well with long-range interaction. Specifically, we examined how the properties of the 1D BJJ dynamics depend on the range of the inter-atomic interaction. The symmetric double well $V_T(x)$ is constructed by fusing the two harmonic potential $V_{\pm}(x) = \frac{1}{2}(x \pm 2)^2$ by a quadratic polynomial $\frac{3}{2}(1 - x^2)$ in the region $|x| \leq 0.5$. We define the width of the double well as the separation between the two local minima of $V_T(x)$ given by $l = 4$. The Rabi oscillations in the double well sets the time scale for the dynamics, $t_{Rabi} = \frac{2\pi}{\Delta E} = 132.498$, where ΔE is the energy difference between the ground state and the first excited state of a single particle in the trap.

We start by preparing a BEC of N interacting bosons in the ground state of the left well $V_+(x)$ at $t < 0$. At $t \geq 0$, the system is allowed to evolve in time in the double well $V_T(x)$. As discussed above, the inter-atomic interaction is chosen as $W(x_j - x_k) = \frac{\lambda_0}{\sqrt{(|x_j - x_k|/D)^{2n} + 1}}$ of half-width D with $n = 3$. The strength of interaction λ_0 corresponds to the mean-field interaction parameter $\Lambda = \lambda_0(N - 1)$. We tune the range D of the interaction for different interaction parameters Λ to study the impact of the long-range tail of the interaction on the BJJ dynamics. For all values of D studied here, the peak of the density appears at the centre of the well. This implies that the tail of the interaction governs the dynamics.

We first consider the time evolution of the survival probability in the left well, $p_L(t) = \int_{-\infty}^0 dx \frac{\rho(x;t)}{N}$, of the BEC in the 1D BJJ. For $\Lambda = 0.01$, it has been earlier shown that even for a system with $N = 1000$ bosons interacting via a contact δ -interaction, the effective interaction is sufficiently weak such that the many-body and mean-field results for the time evolution of the density per particle and $p_L(t)$ coincide [21]. Accordingly, here we compute $p_L(t)$ for various D with the mean-field theory and compare them in Fig. 1(a). We find that for such a weak interaction, the system performs full tunnelling oscillations back and forth between the two wells irrespective of the range of the interaction, and all the curves practically overlap with each other though slight deviations appear at long times. This implies that there is no pronounced impact of the long-range tail of the interaction on the dynamics for such an interaction parameter. The many-body calculations also confirm the

same as can be seen from Fig. 1 (b) where we present the many-body results for $N = 10,000$. It is known that in the $N \rightarrow \infty$

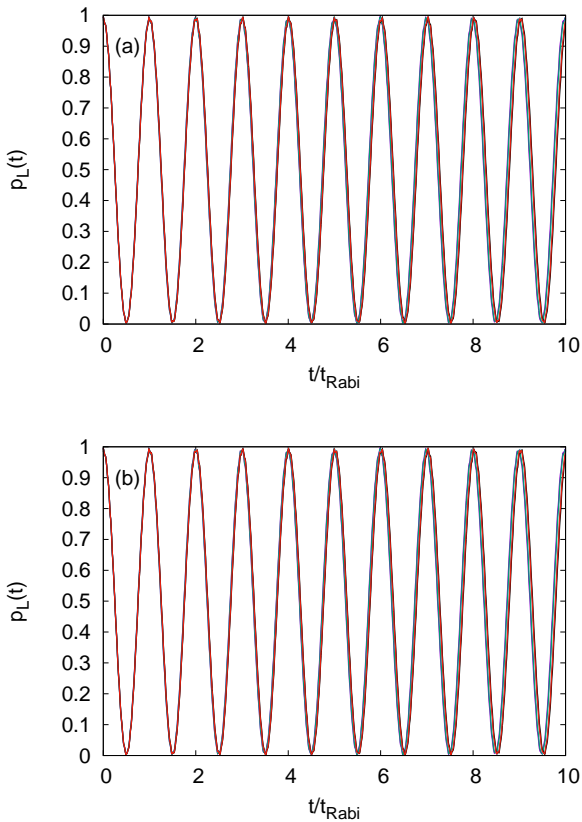


Figure 1: (color online) Time evolution of the survival probability $p_L(t)$ in the left well for various ranges D of the interaction for $\Lambda = 0.01$. In (a) the mean-field results are shown while in (b) MCTDHB results with $M = 2$ orbitals and $N = 10000$ bosons are shown. The magenta curves correspond to $D = l/8$, green curves represent $D = l/4$, blue curves present $D = l/2$, black curves correspond to $D = 3l/4$ and the red curves depict the result for $D = l$; l being the separation between the two local minima of the double-well trap. See text for further details. The quantities shown are dimensionless.

limit, keeping Λ fixed, the energy per particle and density per particle of the system converge to the corresponding mean-field Gross-Pitaevskii (GP) results [56], despite the difference between the many-body and GP wave functions [57, 58] and the many-body effects for these quantities, if any, would already be erased for large N . Similar results hold for the dynamics also [59]. Therefore we have also repeated our many-body calculation with smaller number of particles, viz. $N = 100$ and $N = 1000$ bosons. We plot our results in Fig. 2. We find a competition between the effects of the long-range tail and the confining double-well trap. For $D \ll l$, all the results for different N practically fall on top of each other. However, as D increases we observe a slight damping in the oscillations of $p_L(t)$ till $D = l/2$ when the damping effect is most prominent. Also, over the same time period, the damping is enhanced for smaller N . For larger D , this effect fades away and finally for $D \geq l$, it completely disappears and the mean-field picture is restored. Further, even though the amplitude of the oscillations

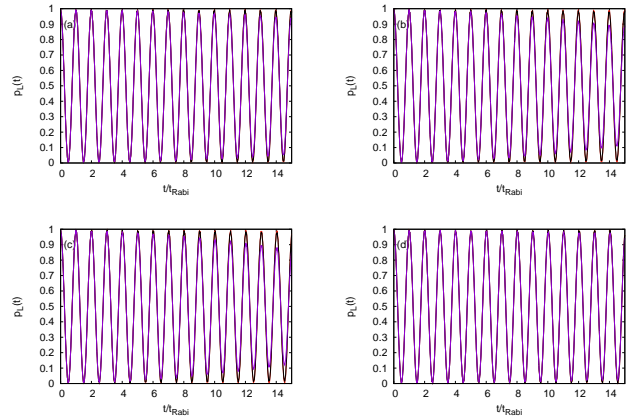


Figure 2: (color online) Time evolution of the survival probability $p_L(t)$ in the left well for various N and a fixed range D of the interaction: (a) $D = l/8$, (b) $D = l/4$, (c) $D = l/2$ and (d) $D = l$. The interaction parameter is $\Lambda = 0.01$. In each panel, the red smooth curve corresponds to $N = 10000$ bosons, black curve to $N = 1000$ bosons and magenta to $N = 100$ bosons. The quantities shown are dimensionless.

is damped for smaller N , the frequency of the oscillations is practically unaffected in all cases and is approximately equal to the Rabi frequency. This implies that the effective interaction is very weak for $\Lambda = 0.01$ and the mean-field limit is attained already for $N = 10,000$ particles as far as $p_L(t)$ is concerned.

In order to understand the damping of oscillations of $p_L(t)$ better, we study the depletion f of the system for all three cases. In Fig. 3 (a) we plot the depletion of the BEC with $N = 10,000$ bosons for various D . We find that for such a small interaction parameter Λ the depletion is negligible and the system is essentially fully condensed irrespective of D . Even then, we find the depletion to increase with D up to $D = l/2$. This implies that the presence of the long-range tail in the interacting potential basically enhances the effect of the interaction up to $D = l/2$. Moreover, there is a correspondence between the damping of the density oscillations and the enhancement of the depletion [see Fig. 2]. In Fig. 3(b) we plot the depletion of the BEC with different N for $D = l/2$. We observe that for a smaller number of bosons, the system becomes more depleted and therefore a more pronounced decay of the oscillations of $p_L(t)$ emerges.

The variance of any operator depends on the actual number of depleted atoms and is a sensitive probe for many-body correlations. It can have a large deviation in comparison with the mean-field theory even when only one out of a million atoms is out of the condensed mode [60]. The many-body position variance per particle $\frac{1}{N}\Delta_X^2$ of a BJJ and the respective position-momentum uncertainty product have been found to already deviate from the mean-field result even for such a weak ($\Lambda = 0.01$) interaction strength [21]. So, it can serve as a better probe to investigate how the many-body correlations are affected in the system due to the presence of the long-range tail in the interaction. Moreover, in Fig. 3(a) we observe that the curves of the depletion for different D are shifted vertically from each other suggesting that for a given N , the total number of atoms residing in higher natural orbitals depends on the

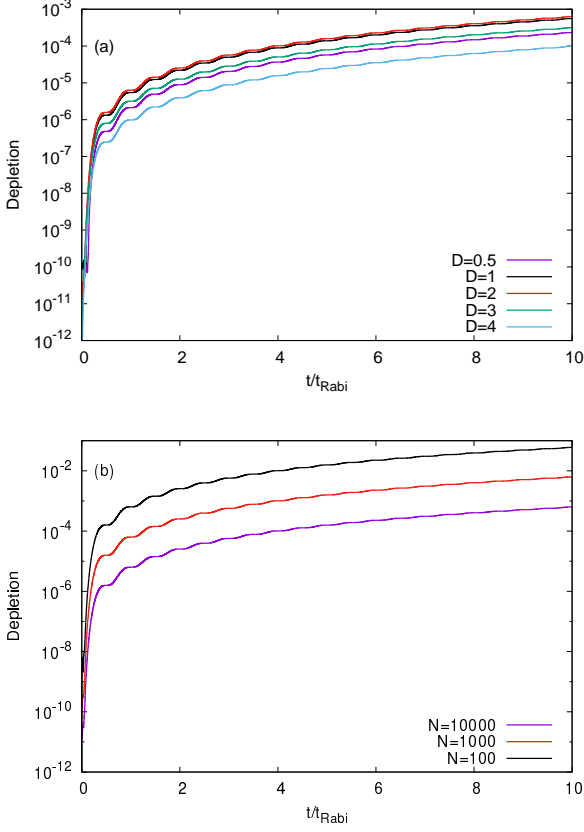


Figure 3: (color online) (a) The depletion per particle of the condensate as a function of time corresponding to Fig. 1(b). (b) The depletion of the condensate with $N = 10,000$ bosons corresponding to Fig. 2(c). The respective color code of the curves is explained in each panel. The quantities shown are dimensionless.

range of the interaction D . Therefore, the variance of an operator is expected to exhibit strong dependence on D . Thus, next we consider the variance per particle of the many-body position operator $\hat{X} = \sum_{j=1}^N \hat{x}_j$ of the system which can be expressed as follows [21, 60]

$$\begin{aligned}
\frac{1}{N} \Delta_{\hat{X}}^2 &= \frac{1}{N} (\langle \Psi | \hat{X}^2 | \Psi \rangle - \langle \Psi | \hat{X} | \Psi \rangle^2) \\
&= \int d\mathbf{r} \frac{\rho(\mathbf{r})}{N} x^2 - N \left[\int d\mathbf{r} \frac{\rho(\mathbf{r})}{N} x \right]^2 \\
&+ \sum_{jpkq} \frac{\rho_{jpkq}}{N(N-1)} \cdot (N-1) \int d\mathbf{r}_2 \phi_j^{*NO}(\mathbf{r}_1) \phi_p^{*NO}(\mathbf{r}_2) \\
&\quad \times x_1 x_2 \phi_k^{NO}(\mathbf{r}_1) \phi_q^{NO}(\mathbf{r}_2).
\end{aligned} \tag{8}$$

In Fig. 4, we plot the variance of the many-body position operator of a BEC of $N = 10,000$ bosons for different D . For all cases, $\frac{1}{N} \Delta_{\hat{X}}^2$ is found to grow in an oscillatory manner, at least for a few Rabi cycles. However, the growth rate depends on D in an intricate manner. The variance is found to grow faster with D until $D = l/2$ and then for further increase in D , the growth of $\frac{1}{N} \Delta_{\hat{X}}^2$ becomes slower. Also, even as the maximal

values of $\frac{1}{N} \Delta_{\hat{X}}^2$ grows with time, its minima values always return to approximately zero. Since the system is essentially fully condensed for $\Lambda = 0.01$, in each oscillation the system is practically localized once in each of the two wells leading to near zero values for the minima. The slight deviation from the zero values can be attributed to the finite depth of the double well. On the other hand, as the number of depleted atoms out of the condensate varies with D , the maximal values of the variance over the same period of time and consequently the growth rate vary accordingly (with D). Moreover, as for the survival probability $p_L(t)$, here also the frequency of oscillations is nearly unaffected and is equal to twice the Rabi frequency for the double well.

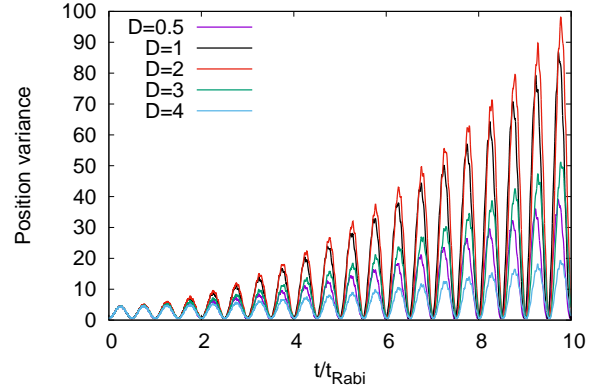


Figure 4: (color online) Time evolution of the position variance per particle $\frac{1}{N} \Delta_{\hat{X}}^2$ for various ranges D of the interaction for $\Lambda = 0.01$ and $N = 10000$ bosons. The quantities shown are dimensionless

To explore the damping in the density oscillations further, we next consider a ten times stronger interaction $\Lambda = 0.1$. Here also, the mean-field result for $p_L(t)$ shows [Fig. 5(a)] that the density of the system tunnels back and forth between the two wells irrespective of the range D of the interaction. However, the frequency of oscillations is found to visibly depend on D , compare to Fig. 1. The frequency is found to somewhat increase with D up to $D = l/2$ and then it slowly decreases for larger D . So, within the mean-field theory, we already observe some effect of the long-range tail of the interaction.

As the mean-field theory cannot describe the collapse and revival of the density oscillations, we also calculate $p_L(t)$ in the left well for a system of $N = 1000$ bosons by the MCTDHB method with $M = 2$ orbitals. We plot the many-body results in Fig. 5(b) for various D . We find that, although the density of the system tunnels back and forth between the two wells, the amplitude of the oscillations decreases with time and eventually it collapses for all $D \leq l$. However, the collapse time t_{collapse} is found to depend on the range D of the interaction. It is observed that the collapse occurs earlier as D increases from a small value up to $D = l/2$ and then t_{collapse} increases for further increase in D . In [20], it has been shown for contact interaction that t_{collapse} decreases for larger Λ with N fixed. This implies that up to $D = l/2$, the presence of the long range tail of the interaction

enhances the effect of the interaction compared to the contact interaction with a similar strength.

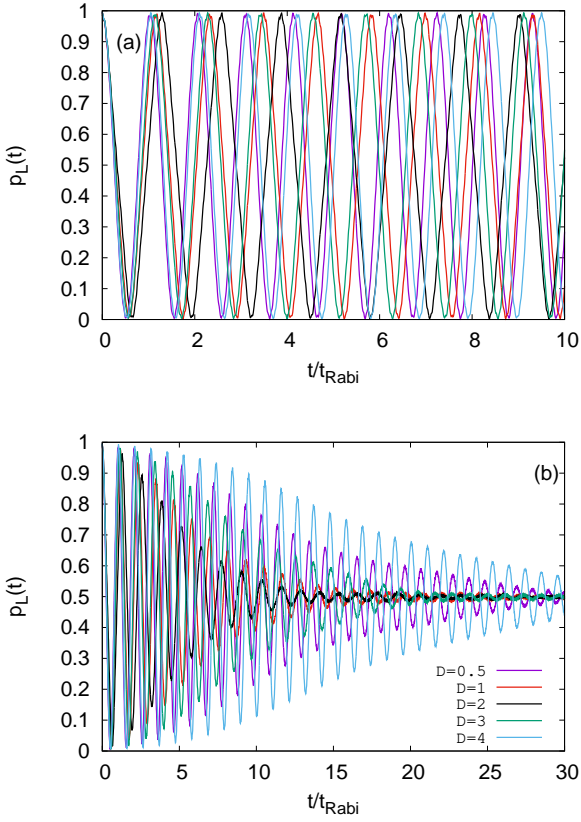


Figure 5: (color online) The time evolution of the survival probability $p_L(t)$ in the left well for various ranges D of the interaction for $\Lambda = 0.1$. In (a) the mean-field results are shown while in (b) MCTDHB results with $M = 2$ orbitals and $N = 1000$ bosons are shown. The color code of the curves is explained in panel (b). The quantities shown are dimensionless.

To further explore the connection between the depletion or fragmentation and the collapse of the density oscillations and its dependence on D , next we study the corresponding natural occupations. We stress that fragmentation of a condensate is a pure many-body phenomena and cannot be described by the mean-field GP theory [61]. In Fig. 6, we plot the natural occupations for different D . Since we started with a practically fully condensed state, initially only one natural orbital is occupied with occupancy $\frac{n_1}{N} \approx 1$ and the corresponding fragmentation $f = \frac{n_2}{N} \approx 0$. However, with time as the condensate starts to tunnel through the barrier, the second natural orbital becomes occupied and the condensate becomes fragmented. The fragmentation f reaches a plateau $f = f_{col}$ around $t_{collapse}$. We found that along with $t_{collapse}$, f_{col} also depends on D . f_{col} first decreases as D is increased starting from a small value till $D = 1/2$, and then for larger D it increases.

Now that the condensate is fragmented, the behavior of the position variance is even more interesting. In Fig. 7, we plot $\frac{1}{N}\Delta_X^2$ as a function of time for various D . Here also we found the variance to increase with time in an oscillatory manner for all

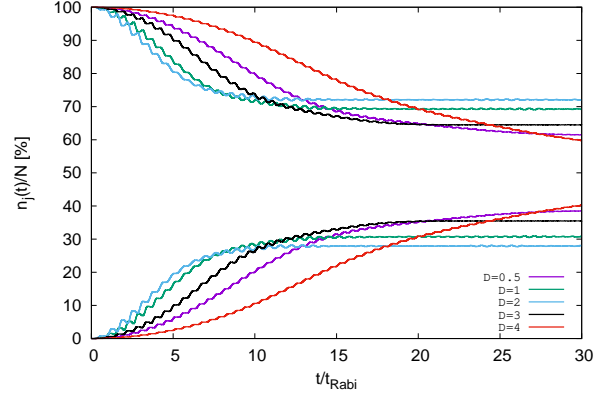


Figure 6: (color online) The fragmentation of the condensate with time for different ranges D for the interaction parameter $\Lambda = 0.1$ and $N = 1000$ bosons. See text for further details. The quantities shown are dimensionless.

D . Moreover, the pace of growth of the variance is again seen to vary with D in a similar manner as in the case of $\Lambda = 0.01$. However, there is a fundamental difference in this case. Now, not only the maxima values but also the minima values of $\frac{1}{N}\Delta_X^2$ increase. This is a consequence of the growing degree of fragmentation of the BEC. Finally at $t \sim t_{collapse}$, as the density oscillations collapse and the fragmentation f reaches a plateau at f_{col} , the variance also exhibits an equilibration-like effect and oscillates about a constant mean value. As f_{col} shifts vertically with D , the actual number of depleted atoms outside the condensate mode also varies with D . Naturally, the mean value about which $\frac{1}{N}\Delta_X^2$ oscillates also moves up and down similarly to f_{col} , see Fig. 7.

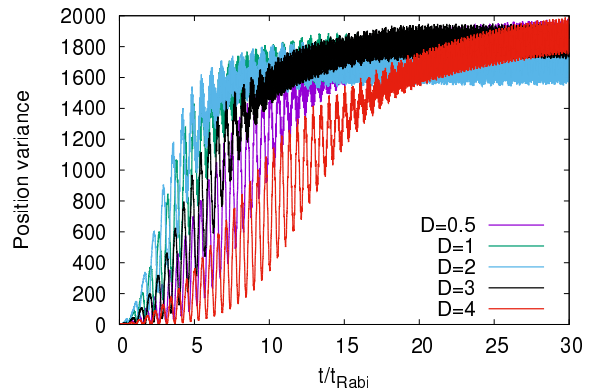


Figure 7: (color online) The time evolution of the position variance per particle $\frac{1}{N}\Delta_X^2$ for various ranges D of the interaction $\Lambda = 0.1$ and $N = 1000$ bosons. For further details see text. The quantities shown are dimensionless.

Last, to examine how the frequency of the density oscillations and the resulting survival probability itself are affected by the range of the interaction more prominently, we increase Λ further. Here we remind that self trapping is an important feature in the BJJ dynamics with δ -interaction [4, 5] when the interaction is stronger than a critical value. In this case, a BEC

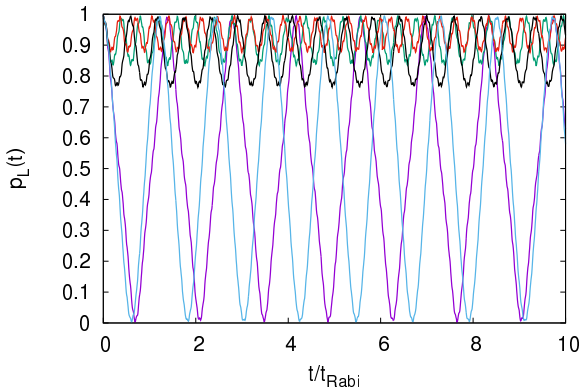


Figure 8: (color online) The time evolution of the survival probability $p_L(t)$ in the left well for various ranges D of the interaction. Only the mean-field results for the interaction parameter $\Lambda = 0.2$ are shown. The magenta smooth curve corresponds to $D = l/8$, green curve represents $D = l/4$, red curve presents $D = l/2$, black curve corresponds to $D = 3l/4$ and the blue curve depicts the result for $D = l$. For further details see text. The quantities shown are dimensionless.

initially localised in one well tends to remain self trapped in that well for more than a few Rabi cycles. So, next, we double the strength of interaction to $\Lambda = 0.2$. In Fig. 8 we plot the mean-field result for $p_L(t)$. We find that now, not only the frequency but also the amplitude of the density oscillations is strongly affected due to the presence of a tail part in the interaction. For small D , similarly to zero-range contact δ -interaction, the system performs full oscillations back and forth between the two wells. However, for larger D , the system exhibits partial self trapping with only up to about 20% tunneling to the other well. Finally, for $D \approx l$, the complete oscillations of $p_L(t)$ is restored. This partial self trapping, as far as we know, is a novel phenomenon found in presence of a long-range tail in the interaction potential already at the mean-field level. We leave it as a future task to investigate the many-body facets of this self-trapping phenomenon.

4. Conclusions

In short, here we have studied how the well known BJJ dynamics is modified in presence of a long-range tail in the interaction potential. We choose a model two-body interaction $W(x_i - x_j)$ with a tunable range D . Such interactions are relevant in view of recent experiments with dressed Rydberg atoms and ultra-cold atoms with a strong dipole moment. The qualitative physics discussed here is expected to remain the same for other repulsive interactions with similar strengths and ranges. We studied the impact of the presence of a tail part in the interaction potential at both the mean-field and many-body levels. For the many-body calculations, we used the MCTDHB method with $M = 2$ orbitals. We have also numerically checked that for our present study, MCTDHB computations with $M = 2$ orbitals are accurate and the convergence of our findings with respect to M time-adaptive orbitals is discussed in the Appendix.

We examined the well-known aspects of BJJ dynamics, viz., density oscillations and their collapse, self trapping, depletion and fragmentation as well as the recently examined position variance. We again stress that, while the density oscillations and self trapping already have some explanations at the mean-field level, the collapse and revival of the density oscillations and fragmentation can only be described by a many-body theory. Moreover, the variance is a sensitive many-body quantity which depends on the actual number of depleted atoms and hence, can deviate from the mean-field result even in the $N \rightarrow \infty$ limit. The impact of the range of the interaction on the dynamics is manifested through several features: the frequency of the density oscillations; depletion; collapse time $t_{collapse}$; fragmentation plateau f_{col} ; maximal and minimal values of the position variance in each cycle of the oscillations and the growth pace of the variance. These are key to our study.

Our work revealed that for a very weak interaction, the system is essentially fully condensed and the density oscillations are practically unaffected by the presence of the tail in the interaction potential. However, as the strength of the interaction increases, its impact gradually becomes prominent. We found an intricate competition between the double-well trap and the range of the interaction. Initially, as the range of the interaction is increased from a small value, it is tantamount to pushing the atoms further away from each other. Naturally, increasing the range of the interacting potential effectively enhances the repulsive interaction. However, as the range of the interaction becomes comparable with the width of the double well trap, the contribution of the confining effect of the trap enhances and the system behaves as if all the atoms are in a constant interaction potential. This, in effect, diminishes the impact of the range of interaction on the dynamics of the system. Therefore, in this study, we have successfully shown that the use of a long-range interaction enriches the physics of the BJJ dynamics. Since BJJ is a paradigmatic device for understanding coherent quantum phenomena with applications in precision measurements [62] and sensing [63], our present study is of fundamental importance.

Acknowledgement

This paper is dedicated to Professor Hans-Dieter Meyer, a dear colleague and friend, on the occasion of his 70th birthday. This research was supported by the Israel Science Foundation (Grant No. 600/15). We are grateful to Shachar Klaiman and Alexej Streltsov for discussions. Computation time on the High Performance Computing system Hive of the Faculty of Natural Sciences at the University of Haifa and on the Cray XC40 system Hazelhen at the High Performance Computing Center Stuttgart (HLRS) is gratefully acknowledged. SKH gratefully acknowledges the continuous hospitality of the Lewiner Institute for Theoretical Physics (LITP) at the Department of Physics, Technion - Israel Institute of Technology.

Appendix A. MCTDHB computations and their accuracy

As already discussed in Sec. 2, the ansatz in MCTDHB is taken as the superposition of M orbitals which are determined by a time-dependent variational principle. In this connection, we would like to mention that in the limit $M \rightarrow \infty$ the set of permanents $\{|\vec{n}; t\rangle\}$ spans the complete N -boson Hilbert space and thus expansion (2) is exact. On the other hand, for $M = 1$ we get back the well-known GP equation. However, in actual numerical calculations we have, of course, to limit the size of the Hilbert space exploited. By allowing also the permanents to be time-dependent we can use much shorter expansions than if only the expansion coefficients are taken to be time-dependent, thus leading to a significant computational advantage.

In our numerical calculations, the many-body Hamiltonian is represented by 128 exponential discrete-variable-representation grid points (using a Fast Fourier transformation routine) in a box of size $[-10, 10]$. We obtain the initial state for the time propagation - the many-body ground state of the BEC in the left well, by propagating the MCTDHB equations of motion in imaginary time [25, 64]. For our numerical computations we use the numerical implementation in the software Package [65, 66]. We keep on repeating the computation with increasing M until convergence is reached and thereby obtain the numerically-exact results.

As a concrete example, convergence with increasing M of the time-dependent many-particle position variance per particle $\frac{1}{N}\Delta_X^2$ of 1D BJJ is discussed here. As discussed in the text, the many-particle position variance is more sensitive to many-body effects compared to the oscillations in survival probability $p_L(t)$ and the fragmentation f . Hence, convergence of $\frac{1}{N}\Delta_X^2$ with increasing M should also imply the convergence of $p_L(t)$ and f with respect to M ; see also [21, 60].

In Fig. A.9, we have plotted the MCTDHB results for $\frac{1}{N}\Delta_X^2$ of 1D BJJ computed with $M=2, 4$ and 6 orbitals for $\Lambda = 0.1$ and $N = 10$. We see that, similarly to Fig. 7, there is an equilibration-like effect in $\frac{1}{N}\Delta_X^2$ though now the oscillations of $\frac{1}{N}\Delta_X^2$ about a fixed mean value are strongly aperiodic due to the rather small system size. Moreover, it can be seen that all the curves practically lie top on each other for all D . In fact, the MCTDHB results for $M = 4$ and $M = 6$ almost completely overlap each other for all D . Also, as can be seen from Fig. A.9(a) and (d) the overlap between the curves is near perfect for very small D as well as for $D \approx l$. Thus, our MCTDHB computations with $M = 2$ orbitals are already converged and aptly describe the physical behavior of the system, at least for the Λ and period of the dynamics considered here.

Since increasing N , keeping the mean-field parameter Λ fixed, amounts to a weaker interaction strength λ_0 , convergence of our results for $N = 1000$ is actually expected to be better than Fig. A.9. Obviously, it should improve further for the smaller interaction parameter $\Lambda = 0.01$. Indeed, from Fig. 1 we see that the survival probability $p_L(t)$ (and hence, also the density per particle) converges already at the GP level for $\Lambda = 0.01$ and $N = 10,000$.

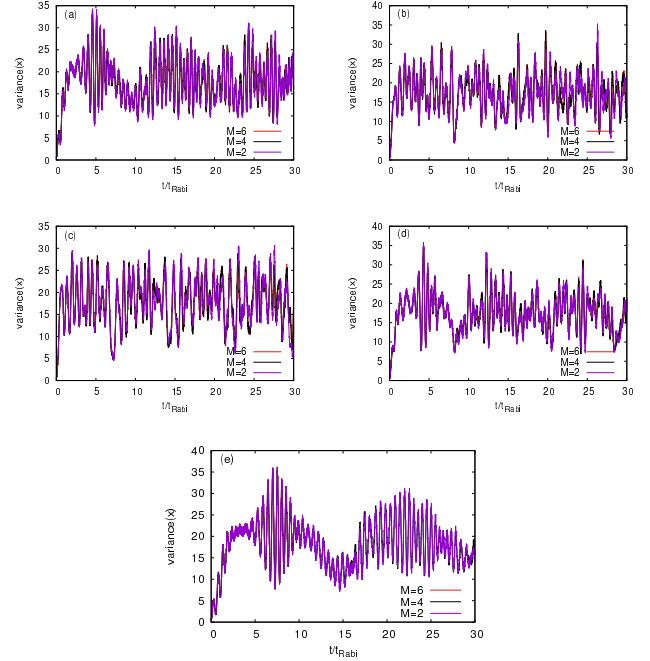


Figure A.9: (color online) Convergence of the time-dependent many-body position variance per particle of a BEC in the one dimensional BJJ with increasing M is shown for $N = 10$ bosons and interaction parameter $\Lambda = 0.1$. (a) $D = l/8$; (b) $D = l/4$; (c) $D = l/2$; (d) $D = 3l/4$ and (e) $D = l$. The results with $M = 2$ accurately describe the variance while the results with $M = 4$ and $M = 6$ orbitals lie on top of each other. See text for further details. The quantities shown are dimensionless.

References

- [1] F. Dalfovo, S. Giorgini, L. P. Pitaevskii and S. Stringari, Rev. Mod. Phys. **71**, 463 (1999).
- [2] S. Zöllner, H.-D. Meyer and P. Schmelcher, Phys. Rev. Lett **100**, 040401 (2008).
- [3] M. Albiez, R. Gati, J. Fölling, S. Hunsmann, M. Cristiani and M. K. Oberthaler, Phys. Rev. Lett. **95**, 010402 (2005).
- [4] G. J. Milburn, J. Corney, E. M. Wright and D. F. Walls, Phys. Rev. A **55**, 4318 (1997).
- [5] A. Smerzi, S. Fantoni, S. Giovanazzi and S. R. Shenoy, Phys. Rev. Lett **79**, 4950 (1997).
- [6] S. Levy, E. Lahoud, I. Shomroni and J. Steinhauer, Nature (London) **449**, 579 (2007).
- [7] S. Raghavan, A. Smerzi, S. Fantoni and S. R. Shenoy, Phys. Rev. A **59**, 620 (1999).
- [8] E. A. Ostrovskaya, Y. S. Kivshar, M. Lisak, B. Hall, F. Cattani and D. Anderson, Phys. Rev. A **61**, 031601(R) (2000).
- [9] Y. Zhou, H. Zhai, R. Lu, Z. Xu and L. Chang, Phys. Rev. A **67**, 043606 (2003).
- [10] C. Lee, Phys. Rev. Lett. **97**, 150402 (2006).
- [11] D. Ananikian and T. Bergeman, Phys. Rev. A **73**, 013604 (2006).
- [12] R. Gati and M. K. Oberthaler, J. Phys. B **40**, R61 (2007).
- [13] G. Ferrini, A. Minguzzi and F. W. J. Hekking, Phys. Rev. A **78**, 023606 (2008).
- [14] V. S. Shchesnovich and M. Trippenbach, Phys. Rev. A **78**, 023611 (2008).
- [15] X. Y. Jia, W. D. Li and J. Q. Liang, Phys. Rev. A **78**, 023613 (2008).
- [16] M. Trujillo-Martinez, A. Posazhennikova and J. Kroha, Phys. Rev. Lett. **103**, 105302 (2009).
- [17] K. Sakmann, A. I. Streltsov, O. E. Alon and L. S. Cederbaum, Phys. Rev. Lett. **103**, 220601 (2009).

- [18] K. Sakmann, A. I. Streltsov, O. E. Alon and L. S. Cederbaum, Phys. Rev. A **82**, 013620 (2010).
- [19] T. Zibold, E. Nicklas, C. Gross and M. K. Oberthaler, Phys. Rev. Lett. **105**, 204101 (2010).
- [20] K. Sakmann, A. I. Streltsov, O. E. Alon and L. S. Cederbaum, Phys. Rev. A **89**, 023602 (2014).
- [21] S. Klaiman, A. I. Streltsov and O. E. Alon, Phys. Rev. A **93**, 023605 (2016).
- [22] G. Spagnolli, G. Semeghini, L. Masi, G. Ferioli, A. Trenkwalder, S. Coop, M. Landini, L. Pezz, G. Modugno, M. Inguscio, A. Smerzi and M. Fattori, Phys. Rev. Lett. **118**, 230403 (2017).
- [23] A. Burchinati, C. Fort and M. Modugno, Phys. Rev. A **95**, 023627 (2017).
- [24] J. Hou, X. -W. Luo, K. Sun, T. Bersano, V. Gokhroo, S. Mossman, P. Engels and C. Zhang, arXiv:1710.06369 (2017).
- [25] A. I. Streltsov, O. E. Alon and L. S. Cederbaum, Phys. Rev. A **73**, 063626 (2006).
- [26] A. Griesmaier, J. Werner, S. Hensler, J. Stuhler and T. Pfau, Phys. Rev. Lett. **94**, 160401 (2005).
- [27] J. Stuhler, A. Griesmaier, T. Koch, M. Fattori, T. Pfau, S. Giovanazzi, P. Pedri and L. Santos, Phys. Rev. Lett. **95**, 150406 (2005).
- [28] M. Lu, N. Q. Burdick, S. H. Youn and B. L. Lev, Phys. Rev. Lett. **107**, 190401 (2011).
- [29] K. Aikawa, A. Frisch, M. Mark, S. Baier, A. Rietzler, R. Grimm and F. Ferlaino, Phys. Rev. Lett. **108**, 210401 (2012).
- [30] M. A. Baranov, Phys. Rep. **464**, 71 (2008).
- [31] T. Lahaye, C. Menotti, L. Santos, M. Lewenstein and T. Pfau, Rep. Prog. Phys. **72**, 126401 (2009).
- [32] S. Giovanazzi, A. Gorlitz and T. Pfau, Phys. Rev. Lett. **89**, 130401 (2002).
- [33] J. Werner, A. Griesmaier, S. Hensler, J. Stuhler, T. Pfau, A. Simononi and E. Tiesinga, Phys. Rev. Lett. **94**, 183201 (2005).
- [34] T. Lahaye, T. Koch, B. Froehlich, M. Fattori, J. Metz, A. Griesmaier, S. Giovanazzi and T. Pfau, Nature (London) **448**, 672 (2007).
- [35] P. Bader and U. R. Fischer, Phys. Rev. Lett. **103**, 060402 (2009).
- [36] A. I. Streltsov, Phys. Rev. A **88**, 041602(R) (2013).
- [37] U. R. Fischer, A. U. J. Lode and B. Chatterjee, Phys. Rev. A **91**, 063621 (2015).
- [38] N. Henkel, F. Cinti, P. Jain, G. Pupillo and T. Pohl, Phys. Rev. Lett. **108**, 265301 (2012).
- [39] L. Santos, G. V. Shlyapnikov, P. Zoller and M. Lewenstein, Phys. Rev. Lett. **85**, 1791 (2000).
- [40] O. I. Streltsov, O. E. Alon, L. S. Cederbaum and A. I. Streltsov, Phys. Rev. A **89**, 061602(R) (2014).
- [41] J. E. Johnson and S. L. Rolston, Phys. Rev. A **82**, 033412 (2010).
- [42] N. Henkel, R. Nath and T. Pohl, Phys. Rev. Lett. **104**, 195302 (2010).
- [43] M. D. Girardeau and E. M. Wright, Phys. Rev. Lett. **84**, 5239 (2000).
- [44] H.-D. Meyer, U. Manthe and L. S. Cederbaum, Chem. Phys. Lett. **165**, 73 (1990).
- [45] U. Manthe, H.-D. Meyer and L. S. Cederbaum, J. Chem. Phys. **97**, 3199 (1992).
- [46] A. I. Streltsov, O. E. Alon and L. S. Cederbaum, Phys. Rev. Lett. **99**, 030402 (2007).
- [47] O. E. Alon, A. I. Streltsov and L. S. Cederbaum, Phys. Rev. A **77**, 033613 (2008).
- [48] P. Kramer and M. Saracento, *Geometry of the time-dependent variational principle* (Springer, Berlin, 1981).
- [49] H.-J. Kull and D. Pfirsch, Phys. Rev. E **61**, 5940 (2000).
- [50] O. Penrose and L. Onsager, Phys. Rev. **104**, 576 (1956).
- [51] P. Nozières, D. Saint James, J. Phys. (France) **43**, 1133 (1982); P. Nozières, in *Bose-Einstein Condensation*, edited by A. Griffin, D. W. Snoke and S. Stringari (Cambridge University Press, Cambridge, England, 1996), p. 15.
- [52] R. W. Spekkens and J. E. Sipe, Phys. Rev. A **59**, 3868 (1999).
- [53] E. J. Mueller, T.-L. Ho, M. Ueda and G. Baym, Phys. Rev. A **74**, 033612 (2006).
- [54] K. Sakmann, A. I. Streltsov, O. E. Alon and L. S. Cederbaum, Phys. Rev. A **78**, 023615 (2008).
- [55] A. I. Streltsov, O. E. Alon and L. S. Cederbaum, Phys. Rev. A **81**, 022124 (2010); A. I. Streltsov, K. Sakmann, O. E. Alon and L. S. Cederbaum, Phys. Rev. A **83**, 043604 (2011).
- [56] E. H. Lieb and R. Seiringer, Phys. Rev. Lett. **88**, 170409 (2002).
- [57] S. Klaiman and L. S. Cederbaum, Phys. Rev. A **94**, 063648 (2016).
- [58] L. S. Cederbaum, Phys. Rev. A **96**, 013615 (2017).
- [59] L. Erdős, B. Schlein, and H.-T. Yau, Phys. Rev. Lett. **98**, 040404 (2007).
- [60] S. Klaiman and O. E. Alon, Phys. Rev. A **91**, 063613 (2015).
- [61] S. Klaiman, N. Moiseyev and L. S. Cederbaum, Phys. Rev. A **73**, 013622 (2006).
- [62] C. Orzel, A. K. Tuchman, M. L. Fenselau, M. Yasuda and M. A. Kasevich, Science **291**, 2386 (2001).
- [63] B. V. Hall, S. Whitlock, R. Anderson, P. Hannaford and A. I. Sidorov, Phys. Rev. Lett. **98**, 030402 (2007).
- [64] A. U. J. Lode, K. Sakmann, O. E. Alon, L. S. Cederbaum and A. I. Streltsov, Phys. Rev. A **86**, 063606 (2012).
- [65] A. I. Streltsov and O. I. Streltsova, MCTDHB-Lab, version 1.5, 2015, <http://www.mctdhlab.com>.
- [66] A. I. Streltsov, L. S. Cederbaum, O. E. Alon, K. Sakmann, A. U. J. Lode, J. Grond, O. I. Streltsova, S. Klaiman, and R. Beinke, The Multiconfigurational Time-Dependent Hartree for Bosons Package, version 3.x, Heidelberg/Kassel (2006-present), <http://mctdhb.org>.